

Myocardium at risk by magnetic resonance imaging: head-to-head comparison of T2-weighted imaging and contrast-enhanced steady-state free precession

Joey F.A. Ubachs¹, Peder Sörensson², Henrik Engblom¹, Marcus Carlsson¹, Stefan Jovinge³, John Pernow², and Håkan Arheden^{1*}

¹Department of Clinical Physiology, Skåne University Hospital, Lund University, Lund SE-22185, Sweden; ²Department of Medicine, Karolinska Institutet, Karolinska University Hospital, Stockholm, Sweden; and ³Department of Cardiology, Skåne University Hospital, Lund University, Lund, Sweden

Received 21 February 2012; accepted after revision 7 April 2012; online publish-ahead-of-print 29 May 2012

Aims

To determine the myocardial salvage index, the extent of infarction needs to be related to the myocardium at risk (MaR). Thus, the ability to assess both infarct size and MaR is of central clinical and scientific importance. The aim of the present study was to explore the relationship between T2-weighted cardiac magnetic resonance (CMR) and contrast-enhanced steady-state free precession (CE-SSFP) CMR for the determination of MaR in patients with acute myocardial infarction.

Methods and results

Twenty-one prospectively included patients with first-time ST-elevation myocardial infarction underwent CMR 1 week after primary percutaneous coronary intervention. For the assessment of MaR, T2-weighted images were acquired before and CE-SSFP images were acquired after the injection of a gadolinium-based contrast agent. For the assessment of infarct size, late gadolinium enhancement images were acquired. The MaR by T2-weighted imaging and CE-SSFP was 29 ± 11 and $32 \pm 12\%$ of the left ventricle, respectively. Thus, the MaR with T2-weighted imaging was slightly smaller than that by CE-SSFP ($-3.0 \pm 4.0\%$; $P < 0.01$). There was a significant correlation between the two MaR measures ($r^2 = 0.89$, $P < 0.01$), independent of the time after contrast agent administration at which the CE-SSFP was commenced (2–8 min).

Conclusion

There is a good agreement between the MaR assessed by T2-weighted imaging and that assessed by CE-SSFP in patients with reperfused acute myocardial infarction 1 week after the acute event. Thus, both methods can be used to determine MaR and myocardial salvage at this point in time.

Keywords

Myocardium at risk • Myocardial salvage • Infarct size • Cardiovascular magnetic resonance • T2-weighted imaging • Contrast-enhanced SSFP

Introduction

Ischaemic heart disease is the leading cause of morbidity and mortality in the Western world. The number of patients who developed an acute myocardial infarction has been increasing exponentially. It was recently estimated that 935 000 new

cases of acute coronary occlusion are identified each year in the USA.¹

Several experimental studies have demonstrated that the region supplied by the occluded coronary artery, also known as myocardium at risk (MaR), is a major independent variable that determines the final infarct size, which in turn is closely related to the clinical

* Corresponding author. Tel: +46 46 173328; fax: +46 46 151769, Email: hakan.arheden@med.lu.se

Published on behalf of the European Society of Cardiology. All rights reserved. © The Author 2012. For permissions please email: journals.permissions@oup.com.

The online version of this article has been published under an open access model. Users are entitled to use, reproduce, disseminate, or display the open access version of this article for non-commercial purposes provided that the original authorship is properly and fully attributed; the Journal, Learned Society and Oxford University Press are attributed as the original place of publication with correct citation details given; if an article is subsequently reproduced or disseminated not in its entirety but only in part or as a derivative work this must be clearly indicated. For commercial re-use, please contact journals.permissions@oup.com

outcome.²⁻⁷ The difference between MaR and infarct size is used to calculate the myocardial salvage index, which is a measurement of the effectiveness of acute interventions aimed at reducing the extent of myocardial infarction.^{8,9} Thus, a feasible and accurate method for determination of MaR is of significant value in clinical studies evaluating the efficiency of cardioprotective therapies.

Cardiovascular magnetic resonance (CMR) imaging is currently considered the reference standard for *in vivo* assessment of myocardial infarction using late gadolinium-enhanced (LGE) imaging.¹⁰ Recently, CMR has also been introduced as a promising method for assessing MaR using T2-weighted imaging¹¹⁻¹⁴ up to 1 week after the acute event.¹⁵ Thus, CMR can be used to calculate the myocardial salvage index by a single CMR imaging session several days after the acute event in a stable clinical setting. Even though T2-weighted imaging is promising for the assessment of MaR, this technique still has certain limitations such as difficulties in distinguishing blood pool from the myocardium, especially in the apical parts of the left ventricle (LV) where hypokinesia and trabeculation cause stagnant blood flow.¹⁶

More recently, a new CMR method for assessment of MaR, referred to as contrast-enhanced steady-state free precession (CE-SSFP), has been introduced.¹⁷ This technique is based on acquisition of time-resolved steady-state free precession images after injection of the gadolinium-based contrast agent and was recently validated against myocardial perfusion single-photon emission computed tomography (SPECT).¹⁷ Still, CE-SSFP has not been compared head-to-head with T2-weighted imaging.

Therefore, the aim of the present study was to explore the relationship between CE-SSFP and T2-weighted imaging with regard to MaR in patients with first-time reperfused acute myocardial infarction.

Methods

Study population

The protocol and procedures were approved by the regional research ethics committee and all patients gave their written consent. Between April 2009 and October 2010, 21 patients (age 59 ± 10 years, 17 males) presenting with first-time acute ST-elevation myocardial infarction (STEMI), due to an occluded coronary artery confirmed by angiography, were prospectively included in the study. All patients were treated with primary percutaneous coronary intervention with coronary stenting, resulting in TIMI grade III flow in the culprit artery. Five patients have been included in an earlier study.¹⁸

Cardiovascular magnetic resonance

One week after admission, CMR was performed using a 1.5 T Philips Intera CV (Philips, Best, The Netherlands). Images were obtained using a five-element chest array surface coil with two anterior and three posterior elements. All subjects were placed in supine position and images were acquired at end-expiratory breath hold with vectorcardiographic gating. Initial scout images were acquired to locate the heart, and a dark-blood T2-weighted triple inversion turbo spin-echo sequence (T2-STIR) was employed to depict the MaR. T2-weighted images were acquired in the short-axis view, covering the LV from the base to the apex. Imaging parameters for the T2-weighted sequence were: echo time, 100 ms; repetition time, 2 heart beats; echo train length, 33; number of averages, 2; inversion time, 180 ms;

image resolution, $1.5 \times 1.5 \times 8$ mm; slice gap, 0 mm. No parallel imaging was performed, but surface coil intensity correction was performed to minimize the signal inhomogeneities due to differences in receiver coil sensitivity.

Acquisition of short-axis, retrospectively gated SSFP cine images, covering the LV from the base to the apex, were initiated within 8 min after the administration of 0.2 mmol/kg extracellular gadolinium-based contrast agent (gadoteric acid, Gd-DOTA; Guerbet, Gothia Medical AB, Billdal, Sweden). These images were referred to as CE-SSFP images (see Supplementary data online, *Movie S1*). Typical image parameters were: echo time, 1.4 ms; repetition time, 2.9 ms; flip angle, 60° ; image resolution, $1.5 \times 1.5 \times 8$ mm; slice gap, 0 mm. No parallel imaging was performed to maximize the signal-to-noise ratio (SNR).

Long- and short-axis LGE images covering the LV were then acquired ~ 15 min after injection of gadolinium. The LGE images were acquired with an inversion-recovery sequence with following image parameters: slice thickness, 8 mm; field of view, 340 mm; flip angle, 15° ; repetition time, 4.2 ms; echo time, 1.3 ms; image resolution, $1.4 \times 1.4 \times 8$ mm; slice gap, 0 mm; parallel imaging with a SENSE factor of 2. The inversion time was adjusted to null the signal from viable myocardium.¹⁹

Image analysis

All CMR images were analysed using the freely available software Segment v1.8 (<http://segment.heiberg.se>).²⁰

The MaR derived from T2-weighted imaging was assessed according to a previously described methodology.¹⁵ In short, endocardial and epicardial borders of the LV were traced in all short-axis slices, followed by manual delineation of the hyperintense regions by two blinded observers. The papillary muscles were excluded from the myocardium. The MaR was then defined as the total amount of hyperintense myocardium in all short-axis slices and expressed as percentage of LV. If present, hypo-intense myocardium within the area of increased signal intensity (microvascular obstruction) was included in the MaR.

The MaR derived from CE-SSFP was also assessed according to previously described methodology.¹⁷ In short, endocardial and epicardial borders of the LV were traced in all short-axis slices in end-diastole and end-systole, followed by manual delineation of the hyperintense regions in both end-diastole and end-systole, by two observers blinded to both the T2-weighted and LGE images. The values of MaR in end-diastole and end-systole were averaged and expressed as a percentage of the LV. The contrast ratio (CR) for the CE-SSFP images was determined for each patient as the mean signal intensity in the MaR divided by the mean signal intensity in remote myocardium.

A slice-by-slice comparison of MaR between T2-weighted imaging and CE-SSFP was also performed for corresponding slice positions.

The infarcted myocardium was automatically quantified from the short-axis LGE images according to a previously described method.²¹ In short, the endocardial and epicardial borders were traced manually with exclusion of the papillary muscles. The LGE myocardium was then defined using a computer algorithm that takes into consideration partial volume effects within the infarcted region. Manual adjustments were made when image artefacts caused misinterpretation by the computer algorithm. If present, a hypointense signal within the area of LGE (microvascular obstruction) was included in the analysis as 100% infarction. Finally, the myocardial infarct size was expressed as a percentage of the LV.

The myocardial salvage index was defined as: $100 * [(MaR - infarct size) / MaR]$, where MaR was assessed by both T2-weighted imaging and CE-SSFP.

The SNR ratio, contrast-to-noise (CNR) ratio and contrast ratio (CR) were determined for T2-weighted, CE-SSFP, and LGE images, respectively. The SNR was calculated as the mean signal intensity within

the affected region (MaR or infarcted myocardium) divided by the standard deviation of signal intensities within a background region of interest. The CNR was calculated as the SNR in the affected region (MaR or infarcted myocardium) – SNR within remote myocardium and CR was calculated as the mean signal intensity in the affected region (MaR or infarcted myocardium) divided by the mean signal intensity in remote myocardium.

Statistics

Continuous variables are presented as mean \pm SD if nothing else specified. Pearson's correlation was used to determine the relationship between T2-weighted imaging and CE-SSFP with regard to MaR and myocardial salvage index. The agreement between T2-weighted imaging and CE-SSFP was expressed as mean difference \pm SD, and the limits of agreement were shown in a Bland–Altman graph as mean \pm 2 SD. The inter-observer variability was expressed as mean difference \pm SD. A paired *t*-test was used to compare the means of the contrast ratio between MaR and remote myocardium for both T2-weighted imaging and CE-SSFP as well as difference in MaR by T2-weighted imaging and CE-SSFP. SPSS version 17.0 software package (Chicago, IL, USA) was used for analysis. Results with a *P*-value of <0.05 were considered statistically significant.

Results

In 59% (12 of 21) of the patients, the right coronary artery (RCA) was the culprit vessel and in 29% (6 of 21) of the patients, the left anterior descending coronary artery (LAD) was the culprit vessel. Furthermore, 2 patients presented with an occlusion of the left circumflex coronary artery and 1 patient had a left main occlusion. In all patients, T2-weighted imaging and CE-SSFP identified the MaR in the same perfusion territory and in concordance with angiography. *Figure 1A* shows an example of multi-slice short-axis images from the base to the apex demonstrating MaR by T2-weighted imaging and CE-SSFP as well as myocardial infarction by LGE, in one patient with an occlusion in the left anterior descending coronary artery. For one patient, myocardial infarct size could not be determined due to poor LGE image quality resulting from frequent arrhythmias. Another patient had a clinical history of a prior infarction in a coronary territory different from that supplied by the current culprit vessel. This patient had no signs of infarction by LGE imaging in the part of the myocardium previously reported to be infarcted. Therefore, this patient was included in the present study.

Myocardium at risk

A region with increased signal intensity by T2-weighted imaging and CE-SSFP was observed in all patients, yielding a mean MaR of $29 \pm 11\%$ (range 12–65) and $32 \pm 12\%$ (range 8–70) of the LV, respectively (*Table 1*).

Figure 1B shows three examples of the agreement of the MaR by T2-weighted imaging and CE-SSFP. Another example including the cine CE-SSFP can be seen in Supplementary data online, *Movie S1*. *Figure 2A* shows a scatter plot indicating the relationship between T2-weighted imaging and CE-SSFP (mean of two observers). There was a strong correlation between the two methods ($r^2 = 0.89$, $P < 0.01$). *Figure 2B* shows the limits of agreement between T2-weighted imaging and CE-SSFP, demonstrating a bias of

$-3.0 \pm 4.0\%$ of the LV ($P < 0.01$). For the slice-by-slice comparison, r^2 was 0.69 ($P < 0.01$; $y = 0.98x + 0.61$) with a bias of $-1.8 \pm 16\%$ per slice.

Figure 3A shows the relationship between time after contrast agent administration at which the CE-SSFP image acquisition was commenced (2–8 min) and the difference between T2-weighted imaging and CE-SSFP for the assessment of MaR. The CE-SSFP

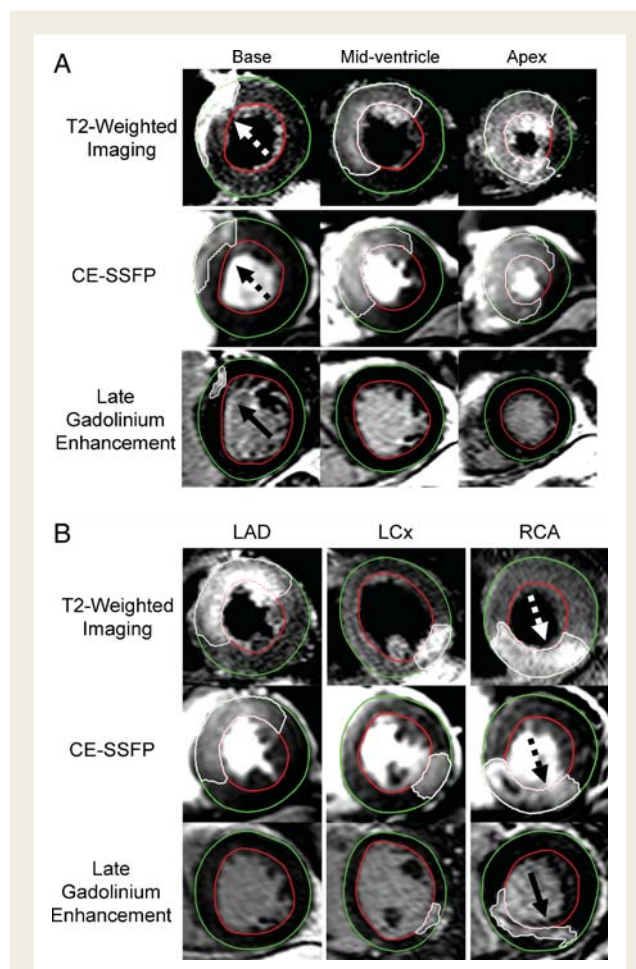


Figure 1 The myocardium at risk by T2-weighted imaging and CE-SSFP, and the infarct size by late gadolinium enhancement. (A) T2-weighted, CE-SSFP, and late gadolinium-enhanced short-axis images at the corresponding LV levels in a patient with a reperused left anterior descending coronary artery occlusion. (B) Single corresponding mid-ventricular short-axis images from a patient with an occlusion in the left anterior descending coronary artery (LAD), left circumflex coronary artery (LCx), and the right coronary artery (RCA), respectively. The epicardium is traced in green and the endocardium is traced in red. The hyperenhanced regions constituting the myocardium at risk (dashed arrows) and the infarcted myocardium (solid arrows) are traced in white. Note the similarity in location and the extent of the affected region between T2-weighted imaging and CE-SSFP. Also note the significantly smaller infarction compared with the myocardium at risk indicating a significant myocardial salvage accomplished by the acute reperfusion therapy. CE-SSFP, contrast-enhanced steady-state free precession.

Table 1 Myocardium at risk, infarct size and myocardial salvage index for each patient

Case no.	Culprit vessel	Myocardium at risk by T2W (%)			Myocardium at risk by CE-SSFP (%)			Infarct size by LGE (%)			Myocardial salvage index (%) by	
		Obs 1	Obs 2	Mean	Obs 1	Obs 2	Mean	Obs 1	Obs 2	Mean	T2W	CE-SSFP
1	LM	65	60	63	70	66	68	49	43	46	26	32
2	LAD	33	27	30	43	34	39	9	10	10	70	76
3	LAD	19	20	20	35	28	32	5	6	6	72	83
4	RCA	39	23	31	24	37	31	23	24	24	24	23
5	RCA	22	20	21	19	23	21	6	6	6	71	71
6	RCA	38	38	38	33	44	39	33	32	33	15	16
7	LAD	43	42	43	42	46	44	— ^a	— ^a	— ^a	— ^a	— ^a
8	RCA	27	28	28	32	32	32	16	14	15	44	52
9	RCA	22	12	17	21	29	25	1	1	1	93	95
10	LAD	47	44	46	46	41	44	25	22	24	49	46
11	RCA	33	31	32	30	30	30	12	10	11	65	63
12	RCA	14	12	13	8	10	9	5	9	7	47	23
13	LAD	38	31	35	44	40	42	21	21	21	38	49
14	LAD	36	28	32	38	35	37	3	3	3	92	93
15	LCX	17	14	16	17	18	18	8	7	8	52	57
16	RCA	30	27	29	30	28	29	11	12	12	60	60
17	LCX	32	12	22	31	19	25	4	4	4	82	84
18	RCA	26	25	26	29	25	27	11	13	12	52	55
19	RCA	30	20	25	27	29	28	7	7	7	73	76
20	RCA	37	31	34	36	38	37	19	16	18	49	53
21	RCA	23	20	22	26	27	27	12	14	13	38	50

CE-SSFP, contrast-enhanced steady state free precession; LAD, left anterior descending; LGE, late gadolinium enhancement; LM, left main; LV, left ventricle; Obs, observer; RCA, right coronary artery; T2W, T2-weighted imaging.

^aInfarct size could not be assessed due to poor image quality related to frequent arrhythmias.

imaging lasted for 2–4 min and the latest image was acquired 12 min after contrast agent administration. There was no change in the relationship between the two techniques as a function of time after contrast agent administration. This is illustrated in a patient with an LAD occlusion in *Figure 3B*.

In six patients, cine SSFP short-axis imaging was also performed prior to contrast agent administration. In five of six patients, no hyperenhancement was seen, which is illustrated in *Figure 3B*. For one patient, a slight hyperenhancement with indistinct borders was found within the MaR.

SNR within the MaR was 156 ± 7 and 132 ± 10 for the T2-weighted imaging and CE-SSFP, respectively (mean \pm SEM). The CNR was 58 ± 3 and 27 ± 6 for the T2-weighted imaging and CE-SSFP, respectively (mean \pm SEM). The contrast ratio between MaR and remote myocardium for T2-weighted imaging was 1.7 ± 0.3 compared with 1.5 ± 0.4 for CE-SSFP, which was not statistically significant different ($P > 0.05$).

The interobserver variability was $5.0 \pm 5.4\%$ of the LV for T2-weighted imaging and $0.1 \pm 6.2\%$ of the LV for CE-SSFP.

Myocardial salvage index

The mean infarct size by LGE was $14 \pm 11\%$ (range 1–49) of the LV. The interobserver variability was $0.3 \pm 2.2\%$ of the LV. The

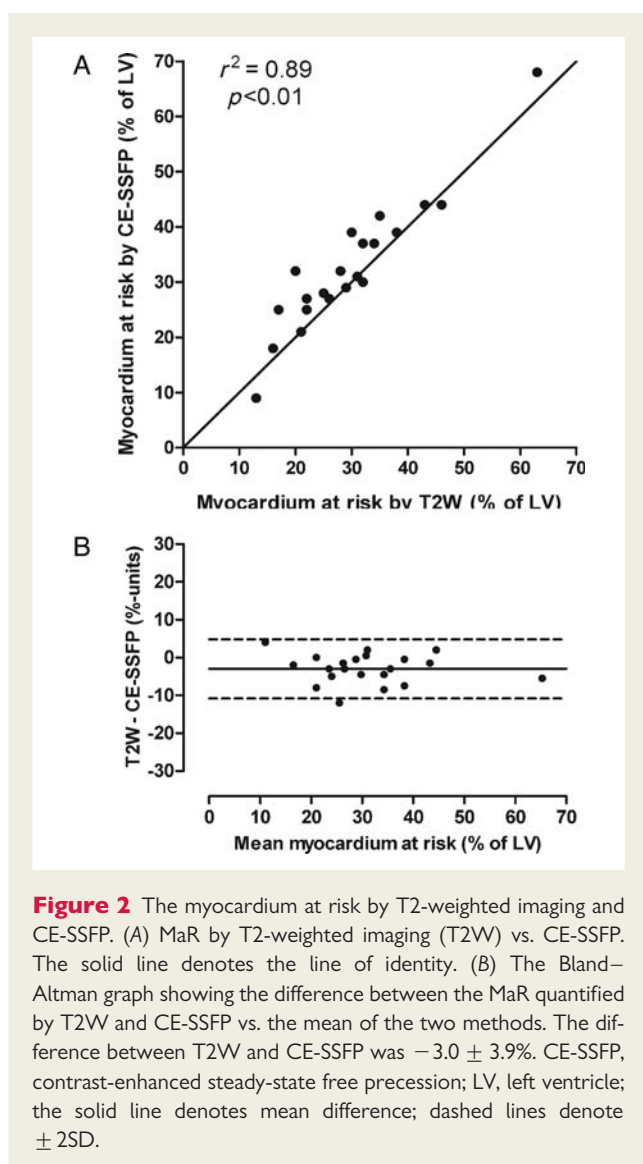
infarct size was smaller in all patients when compared with MaR assessed by T2-weighted imaging ($P < 0.01$) and CE-SSFP ($P < 0.01$).

Comparison of the infarct size by LGE in relation to MaR determined by T2-weighted imaging and CE-SSFP yielded a myocardial salvage index of $56 \pm 22\%$ (range: 15–93) and $58 \pm 23\%$ (range: 16–95), respectively (*Figure 4, Table 1*). There was a significant correlation ($r^2 = 0.89$, $P < 0.01$) between the myocardial salvage index measured by the two methods (*Figure 5*), with an insignificant bias of $-2.3 \pm 7.4\%$ of the LV ($P = 0.20$).

For the LGE images, the SNR within the infarction was 115 ± 12 and the CNR was 73 ± 8 . Note that the LGE images were acquired using parallel imaging increasing the noise levels in these images. The contrast ratio between remote and infarcted myocardium was 2.9 ± 0.8 , which was significantly higher than for T2-weighted imaging and CE-SSFP ($P < 0.001$).

Discussion

This study explored the agreement between MaR assessed by T2-weighted imaging and MaR assessed by CE-SSFP. The agreement was shown to be good, both for the assessment of MaR and myocardial salvage index.



Both T2-weighted imaging and CE-SSFP have previously been validated against MaR assessed by myocardial perfusion SPECT, with a mean difference of -2.3 ± 5.7 and $0.5 \pm 5.1\%$ of the LV, respectively.^{17,22} In accordance with these results, the present study found a small bias of $-3.0 \pm 4.0\%$ when T2-weighted imaging was compared with CE-SSFP. This is, however, the first time these two techniques have been compared head-to-head which is important in order to ensure that both techniques can be used interchangeably in clinical cardioprotection trials using myocardial salvage as endpoint.

The correlation between MaR by T2-weighted imaging and CE-SSFP was not as strong for the slice-by-slice comparison as for the global measure of MaR normalized to the entire LV. As the heart rate varies, the timing within the cardiac cycle at which the T2-weighted image is acquired varies resulting in difficulties with local registration of the myocardium when comparing the two techniques. Even though the slice position was approximately the same for the two acquisitions, the part of the myocardium depicted may differ due to AV-plane movement during the

cardiac cycle. This is not a problem when comparing global measures of MaR normalized to the entire LV.

More recently, bright-blood T2-weighted sequences have been developed to increase the diagnostic performance of T2 CMR for oedema depiction.^{11,13} In a recent study by Payne *et al.*,¹⁴ dark-blood T2-STIR was shown to underestimate the MaR with $\sim 9\%$ units compared with the recently introduced bright-blood T2-weighted sequence (ACUT₂E).¹¹ It was concluded that ACUT₂E was more accurate for the determination of MaR and myocardial salvage than was dark-blood T2-STIR. Thus, CE-SSFP might be more accurate than dark-blood T2 in the present study since CE-SSFP showed larger MaR and, previously, showed no bias compared with myocardial perfusion SPECT.¹⁷

The pathophysiological basis for the enhanced myocardium observed using T2-weighted imaging is still not completely understood. Following acute coronary occlusion, the ischaemic myocardium shifts from aerobic metabolism to anaerobic glycolysis and ceases to contract. This failure of the energy-regulated membrane channels results in swelling of the myocytes due to influx of water and sodium.²³ Furthermore, reperfusion leads to inflammatory-like response, increasing the amount of extracellular fluid.²⁴ This increased water content in the affected myocardium is likely to explain the increased signal intensity compared with the non-affected myocardium as seen by T2-weighted imaging. Whether the increased water content is predominantly intracellular or extracellular remains to be determined. The ischaemic episode causes post-ischaemic stunning,²⁵ associated with a decreased contractility in the previously ischaemic myocardium. This decreased contractility is likely associated with a decreased lymphatic drainage from this part of the myocardium, which may also contribute to residual increased water content 1 week after the acute event.

The mechanisms behind the enhanced myocardium observed in CE-SSFP are not completely known either. The contrast in SSFP images is dependent on the T2/T1 ratio.²² In the presence of paramagnetic gadolinium, the T1 for the surrounding tissue is shortened. This is utilized for infarct visualization in T1-weighted inversion-recovery LGE imaging, where the concentration of an extracellular gadolinium-based contrast agent is increased due to an increased distribution volume in ischaemically injured myocardium.^{26–29} It has been shown that even reversibly injured myocardium within the MaR has an increased distribution volume in the acute phase after an ischaemic episode.^{28,29} Hence, the T2/T1 ratio in the entire MaR, including both reversible and irreversible injured myocardium, is affected by the presence of gadolinium. This might explain the increased signal intensity in the MaR seen by CE-SSFP. Furthermore, it has been shown that the relationship between the change in T1-relaxation rates before and after contrast agent administration ($\Delta R1$) in different parts of the myocardium (remote, salvaged, and infarcted) in relation to $\Delta R1$ in blood ($\Delta R1$ ratios) remains constant from 4 to 29 min after contrast agent administration in acute myocardial infarction.²⁹ These earlier findings indicate that the rate of exchange of contrast agent between the myocardium (normal and injured) and the blood pool is constant and much faster than the clearance rate in the kidneys during the first 30 min after contrast agent administration. Ugander *et al.*³⁰ recently showed similar findings supporting this concept using T1 mapping before and after contrast

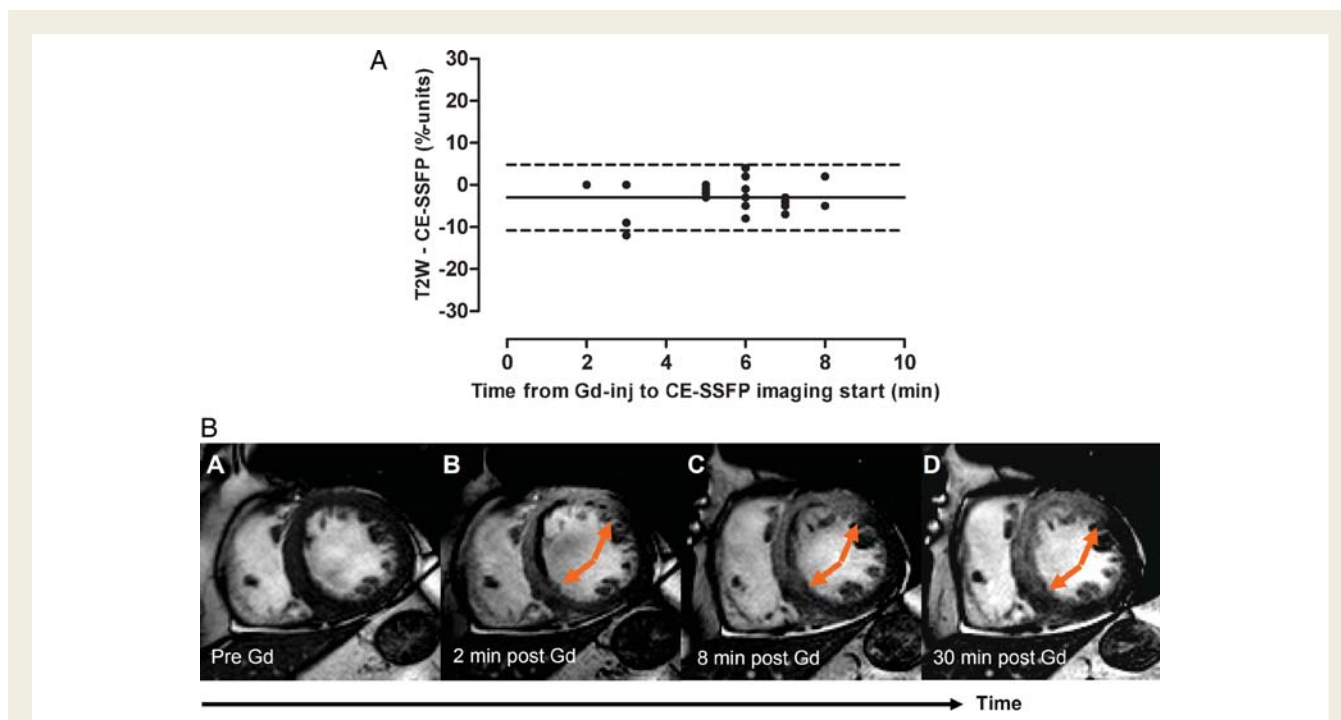


Figure 3 The MaR by CE-SSFP as a function of time after Gd administration. (A) The difference between MaR by T2-weighted imaging and CE-SSFP as a function of time after contrast agent administration at which the CE-SSFP imaging was commenced. The relationship between MaR by T2-weighted imaging and CE-SSFP was not affected by increased time after contrast injection at which the CE-SSFP was commenced. (B) An example of a patient with an infarction within the LAD territory. It is shown that no hyperenhancement could be seen prior to Gd administration (A), whereas a hyperenhanced region was seen 2, 8, and 30 min after Gd administration (B–D). Note that the extent of hyperenhancement did not change during the first 30 min after Gd injection (arrows). CE-SSFP, contrast-enhanced steady-state free precession; Gd-inj, gadolinium contrast agent injection; T2W, T2-weighted imaging; solid line, mean difference; dashed lines = \pm 2SD.

administration in experimentally induced infarction. Thus, this can explain why the relationship between MaR assessed by T2-weighted imaging and CE-SSFP did not change with time after contrast agent administration in the present study (Figure 3) and why the timing of CE-SSFP after contrast agent administration is not critical. Therefore, CE-SSFP could potentially be added to clinical protocols so that cine imaging is acquired after contrast agent administration for the assessment of LV function and MaR.

One advantage with CE-SSFP imaging is that this technique is based on a multi-phase acquisition throughout the cardiac cycle. This enables tracking of the MaR and myocardial borders in multiple time frames (see Supplementary data online, *Movie S1*), making delineation of both MaR and myocardial borders more robust. In the present protocol, MaR in the CE-SSFP images were traced in both end-systole and end-diastole and averaged. Another situation where CE-SSFP could be advantageous is when limited time for scanning is available, due to heavy clinical load or an unstable patient. In such a situation, gadolinium can be injected prior to the examination and the imaging protocol can be shortened since LV dimensions/function and MaR can be assessed from the same set of images. On the other hand, T2-weighted imaging for the determination of MaR can be performed in those patients where administration of a gadolinium-based contrast agent is contraindicated. Thus, there are several advantages of having access to more than one method for

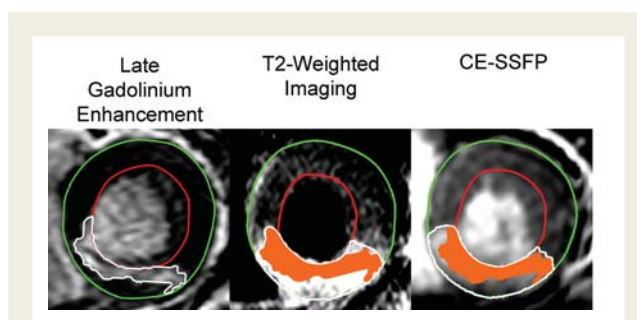
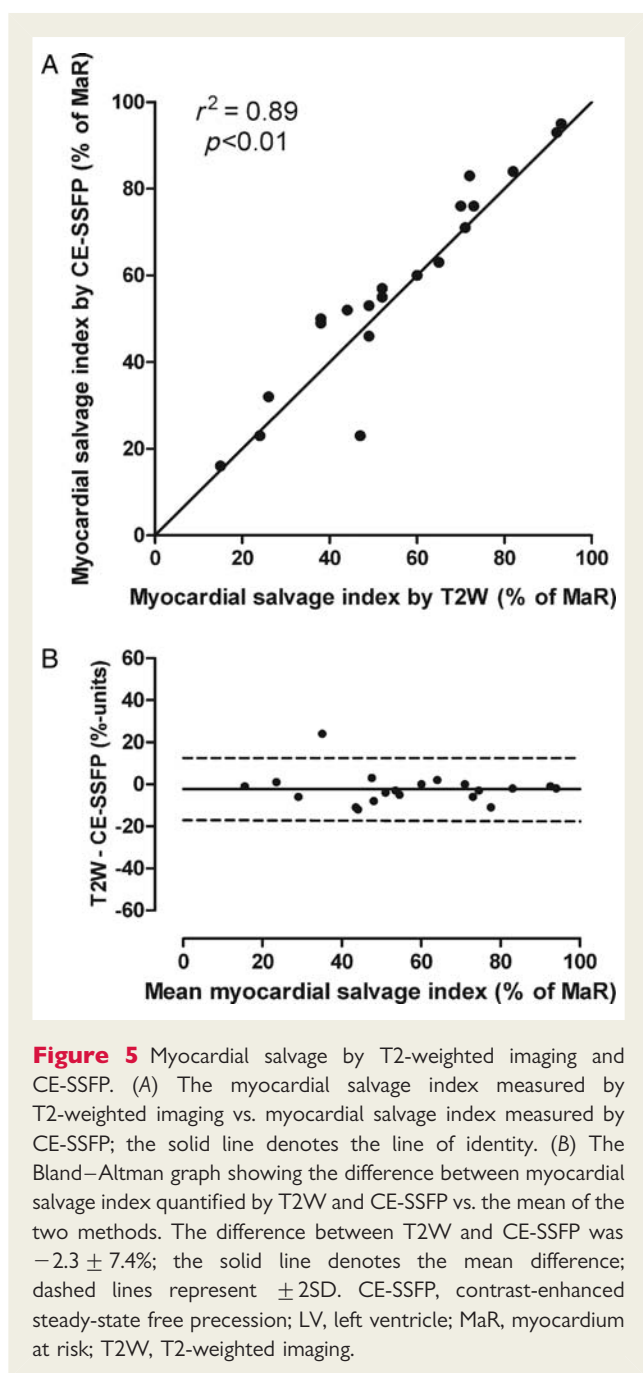


Figure 4 Graphical display of myocardial salvage. Mid-ventricular short-axis slices in a patient with a right coronary artery occlusion. The epicardium is traced in green, the endocardium is traced in red, and the affected region is traced in white. The infarcted myocardium on the late gadolinium-enhanced image is superimposed (orange) on the myocardium at risk within the T2-weighted image and the CE-SSFP image. The non-coloured part of the myocardium at risk defines the salvaged myocardium. For this patient, T2-weighted imaging and CE-SSFP showed 52 and 55% myocardial salvage, respectively. CE-SSFP, contrast-enhanced steady-state free precession.

determination of MaR by CMR and we recommend both T2-weighted imaging and CE-SSFP to be implemented in the imaging protocol. Owing to the relatively small differences in



signal intensity between MaR and remote myocardium, we recommend not to use parallel imaging when acquiring CE-SSFP images as this decreases the SNR. No significant difference in the contrast ratio between T2-weighted imaging and CE-SSFP imaging was found in the present study where no parallel imaging was performed.

Study limitations

The present study was performed on a limited number of STEMI patients, all undergoing successful reperfusion. Thus, how this would translate to a non-STEMI population or to patients treated with thrombolytic therapy is not known.

Since only a few female patients were included, gender perspective cannot be evaluated.

No semi-quantitative method was used to determine the MaR by both T2-weighted imaging and CE-SSFP, since the signal intensities of the MaR and the remote myocardium varied between slices and between patients, making it difficult to choose a fixed standard deviation of signal intensities to differentiate MaR from remote myocardium.

Conclusions

There is a good agreement between MaR assessed by T2-weighted imaging and MaR assessed by CE-SSFP in patients with reperfused acute myocardial infarction 1 week after the acute event. Thus, both methods can be used to determine MaR and subsequently myocardial salvage at this point in time.

Supplementary data

Supplementary data are available at *European Heart Journal - Cardiovascular Imaging* online.

Acknowledgements

The authors would like to acknowledge Ann-Helen Arvidsson and Christel Carlander, both with the Lund Cardiac MR Group, for skilful assistance with image acquisition.

Conflict of interest: none declared.

Funding

This study was funded by the Swedish Research Council (521-2008-2461), the Swedish Heart and Lung Foundation, the Medical Faculty at Lund University, Sweden, European Commission FP7 Consortium CardioCell, Region of Scania, Sweden, the Stockholm County Council and Karolinska Institutet/Stockholm County Council Strategic Cardiovascular Program.

References

- Lloyd-Jones D, Adams R, Carnethon M, De Simone G, Ferguson TB, Flegal K et al. Heart disease and stroke statistics—2009 update: a report from the American Heart Association Statistics Committee and Stroke Statistics Subcommittee. *Circulation* 2009;**119**:480–6.
- Jennings RB, Sommers HM, Smyth GA, Flack HA, Linn H. Myocardial necrosis induced by temporary occlusion of a coronary artery in the dog. *Arch Pathol* 1960;**70**:68–78.
- Koyanagi S, Eastham CL, Harrison DG, Marcus ML. Increased size of myocardial infarction in dogs with chronic hypertension and left ventricular hypertrophy. *Circ Res* 1982;**50**:55–62.
- Reimer KA, Ideker RE, Jennings RB. Effect of coronary occlusion site on ischaemic bed size and collateral blood flow in dogs. *Cardiovasc Res* 1981;**15**:668–74.
- Kloner RA, Braunwald E. Observations on experimental myocardial ischaemia. *Cardiovasc Res* 1980;**14**:371–95.
- Lee JT, Ideker RE, Reimer KA. Myocardial infarct size and location in relation to the coronary vascular bed at risk in man. *Circulation* 1981;**64**:526–34.
- Lowe JE, Reimer KA, Jennings RB. Experimental infarct size as a function of the amount of myocardium at risk. *Am J Pathol* 1978;**90**:363–79.
- Friedrich MG, Abdel-Aty H, Taylor A, Schulz-Menger J, Messroghli D, Dietz R. The salvaged area at risk in reperfused acute myocardial infarction as visualized by cardiovascular magnetic resonance. *J Am Coll Cardiol* 2008;**51**:1581–7.
- Hedstrom E, Engblom H, Frogner F, Astrom-Olsson K, Ohlin H, Jovinge S et al. Infarct evolution in man studied in patients with first-time coronary occlusion in comparison to different species—implications for assessment of myocardial salvage. *J Cardiovasc Magn Reson* 2009;**11**:38.

10. Pennell DJ, Sechtem UP, Higgins CB, Manning WJ, Pohost GM, Rademakers FE *et al*. Clinical indications for cardiovascular magnetic resonance (CMR): consensus panel report. *Eur Heart J* 2004;**25**:1940–65.
11. Aletras AH, Kellman P, Derbyshire JA, Arai AE. ACUT2E TSE-SSFP: a hybrid method for T2-weighted imaging of edema in the heart. *Magn Reson Med* 2008;**59**:229–35.
12. Aletras AH, Tilak GS, Natanzon A, Hsu LY, Gonzalez FM, Hoyt RF Jr. *et al*. Retrospective determination of the area at risk for reperfused acute myocardial infarction with T2-weighted cardiac magnetic resonance imaging: histopathological and displacement encoding with stimulated echoes (DENSE) functional validations. *Circulation* 2006;**113**:1865–70.
13. Kellman P, Aletras AH, Mancini C, McVeigh ER, Arai AE. T2-prepared SSFP improves diagnostic confidence in edema imaging in acute myocardial infarction compared to turbo spin echo. *Magn Reson Med* 2007;**57**:891–7.
14. Payne AR, Casey M, McClure J, McGeoch R, Murphy A, Woodward R *et al*. Bright-blood T2-weighted MRI has higher diagnostic accuracy than dark-blood short tau inversion recovery MRI for detection of acute myocardial infarction and for assessment of the ischemic area at risk and myocardial salvage. *Circ Cardiovasc Imaging* 2011;**4**:210–9.
15. Carlsson M, Ubachs JF, Hedstrom E, Heiberg E, Jovinge S, Arheden H. Myocardium at risk after acute infarction in humans on cardiac magnetic resonance: quantitative assessment during follow-up and validation with single-photon emission computed tomography. *JACC Cardiovasc Imaging* 2009;**2**:569–76.
16. Abdel-Aty H, Simonetti O, Friedrich MG. T2-weighted cardiovascular magnetic resonance imaging. *J Magn Reson Imaging* 2007;**26**:452–9.
17. Sorensson P, Heiberg E, Saleh N, Bouvier F, Caidahl K, Tornvall P *et al*. Assessment of myocardium at risk with contrast enhanced steady-state free precession cine cardiovascular magnetic resonance compared to single-photon emission computed tomography. *J Cardiovasc Magn Reson* 2010;**12**:25.
18. Ubachs JF, Engblom H, Erlinge D, Jovinge S, Hedstrom E, Carlsson M *et al*. Cardiovascular magnetic resonance of the myocardium at risk in acute reperfused myocardial infarction: comparison of T2-weighted imaging versus the circumferential endocardial extent of late gadolinium enhancement with transmural projection. *J Cardiovasc Magn Reson* 2010;**12**:18.
19. Simonetti OP, Kim RJ, Fieno DS, Hillenbrand HB, Wu E, Bundy JM *et al*. An improved MR imaging technique for the visualization of myocardial infarction. *Radiology* 2001;**218**:215–23.
20. Heiberg E, Sjogren J, Ugander M, Carlsson M, Engblom H, Arheden H. Design and validation of Segment—freely available software for cardiovascular image analysis. *BMC Med Imaging* 2010;**10**:1.
21. Heiberg E, Ugander M, Engblom H, Gotberg M, Olivecrona GK, Erlinge D *et al*. Automated quantification of myocardial infarction from MR images by accounting for partial volume effects: animal, phantom, and human study. *Radiology* 2008;**246**:581–8.
22. Caravan P. Strategies for increasing the sensitivity of gadolinium based MRI contrast agents. *Chem Soc Rev* 2006;**35**:512–23.
23. Willerson JT, Scales F, Mukherjee A, Platt M, Templeton GH, Fink GS *et al*. Abnormal myocardial fluid retention as an early manifestation of ischemic injury. *Am J Pathol* 1977;**87**:159–88.
24. Maxwell SR, Lip GY. Reperfusion injury: a review of the pathophysiology, clinical manifestations and therapeutic options. *Int J Cardiol* 1997;**58**:95–117.
25. Kloner RA, Bolli R, Marban E, Reinlib L, Braunwald E. Medical and cellular implications of stunning, hibernation, and preconditioning: an NHLBI workshop. *Circulation* 1998;**97**:1848–67.
26. Diesbourg LD, Prato FS, Wisenberg G, Drost DJ, Marshall TP, Carroll SE *et al*. Quantification of myocardial blood flow and extracellular volumes using a bolus injection of Gd-DTPA: kinetic modeling in canine ischemic disease. *Magn Reson Med* 1992;**23**:239–53.
27. Saeed M, Wendland MF, Masui T, Higgins CB. Reperfused myocardial infarctions on T1- and susceptibility-enhanced MRI: evidence for loss of compartmentalization of contrast media. *Magn Reson Med* 1994;**31**:31–9.
28. Arheden H, Saeed M, Higgins CB, Gao DW, Bremerich J, Wyttenbach R *et al*. Measurement of the distribution volume of gadopentetate dimeglumine at echo-planar MR imaging to quantify myocardial infarction: comparison with ^{99m}Tc-DTPA autoradiography in rats. *Radiology* 1999;**211**:698–708.
29. Arheden H, Saeed M, Higgins CB, Gao DW, Ursell PC, Bremerich J *et al*. Reperfused rat myocardium subjected to various durations of ischemia: estimation of the distribution volume of contrast material with echo-planar MR imaging. *Radiology* 2000;**215**:520–8.
30. Ugander M, Oki AJ, Hsu LY, Kellman P, Greiser A, Aletras AH *et al*. Extracellular volume imaging by magnetic resonance imaging provides insights into overt and sub-clinical myocardial pathology. *Eur Heart J* 2012 [Epub ahead of print].